

THE SIDE-RAY SYSTEMS OF COMET BENNETT, 1970 MARCH 7–18

FREEMAN D. MILLER

Department of Astronomy, University of Michigan, Ann Arbor, Michigan 48109-1090

Received 21 February 1992; revised 8 May 1992

ABSTRACT

Photographs of Comet Bennett are available for 13 nights in a period March 7–21. On these nights, the main tail shows no signs of major disruptions; it appears that the photographs represent a period of reasonably quiet interactions between the solar wind with its entrained magnetic field and the comet. On Curtis Schmidt plates taken on 9 nights spanning the interval March 7–18 this interaction included the formation of systems of side rays which are the focus of this investigation. We report on the configuration of these arrays and examine the extent of their conformity to a mutually consistent pattern on the sky, and to the familiar ray-folding phenomenon. The structure of the side-ray systems is then compared with a model of magnetically channeled outflow (MCO) in which rays are considered as tracers of field lines lying in the plane of the interplanetary magnetic field (IMF) at the comet and draped about its head. Projection of the observed rays into the plane of the IMF of each date yields rather implausible ray configurations, but the large angles between the planes of the sky and the IMF indicate the need for analysis of cases of less extreme geometry. The familiar anticorrelation between lengths of side rays and distances from the tail axis is found to be inconsistent with a modified MCO in which the planes of successive rays are random walked about the Sun–Comet line by tangential discontinuities in the IMF. Finally attention is called to the need for magnetohydrodynamic models of side-ray systems when, as in this and other instances, the winding angle of the IMF with respect to the Sun–Comet line is small.

1. INTRODUCTION

Discussions of wide-field images of the plasma tails of comets have dealt for the most part with disturbances of the main tails, such as disconnection events and departures from strict linearity, and on the interpretation of such phenomena in terms of variability of the properties of the solar wind and its associated IMF. In a report on our observations of Comet Halley (Miller & Liller 1986) we reviewed Curtis Schmidt photographs of Comet Bennett and called attention to the period 1970 March 7–18 when, on nine nights of observations, groups of short side rays were common, and no major disturbances of the main tail occurred. Niedner & Brandt (1979) suggested that the appearance of tail rays is strongest at the time of a disconnection event, but this association does not appear to have occurred in the case of Comet Bennett. Ioffe (1985) remarked that orderly ray structure is most likely due to a process that develops during a state of steady flow, and Miller (1988) mentioned that useful information on the interaction of the solar wind with cometary plasma might be drawn from study of orderly systems of side rays. This line of thought is pursued in the present paper.

Seventeen plates of Comet Bennett were taken with the Curtis Schmidt at CTIO between March 7 and 18 inclusive (Table 1). Exposures were from 1 to 15 min on IIA-0 emulsion; plate scales ranged from 52 000 to 67 000 km/mm.

The appearance and activity of the main plasma tail is described briefly in Sec. 2, and the delineation of the forms of 72 side-ray features and the structure of the arrays in Sec. 3. In Sec. 4 we present comparisons of the observa-

tions with a commonly (but not universally) accepted model of the nature of tail-ray systems.

2. THE MAIN PLASMA TAIL

It has been proposed (Ip 1980; Wolff *et al.* 1985) that plasma main tails and side rays are the products of different mechanisms. Since the principal concern of this work is with the latter, this section is limited to describing obvious characteristics of the main tail.

2.1 Tail Structure

Images of the main tail, as projected on the sky plane, range in equivalent length from 6 to 10 mil km, depending on exposure time, atmospheric transparency, and possibly ion production rate. Position angles of the tail axes were needed to define the coordinate systems in which the rays were delineated, and were measured with an uncertainty of 1° to 2°. (In this work the number of observations is usually too small for evaluation of standard statistical errors, and we give either the average absolute deviation, or a more subjective judgement of the “uncertainty.”) Except for one night, the segment of the main tail that defined the tail axis lay beyond the tail rays, and one cannot be sure that the inner tail would have yielded the same position angle. Niedner *et al.* (1978) found two consecutive segments of the tail of Comet Kohoutek of lengths 9 and 5 mil km respectively, inclined to one another by 6°5.

Ershkovich *et al.* (1982) and Niedner *et al.* (1983) discussed observations and models of the flaring angles of the plasma tails of Comets 1973 XII and 1974 III on 2 nights each, finding a maximum flaring angle of 4°. Miller (1979)

TABLE 1. Distance and latitude.

March	Heliocentric	Heliographic
	Distance	Latitude
Date	(AU)	(°)
7.4	0.61	-50
8.4	0.60	-47
9.4	0.59	-44
10.4	0.58	-42
11.4	0.57	-39
12.4	0.57	-36
14.4	0.55	-29
16.4	0.54	-22
18.4	0.54	-15

obtained a mean angle of 4° for the tail of Comet 1969 IX on 11 nights, and for Comet Bennett in the present study a mean of 9° . It is possible that the difference between the flaring angles of Ershkovich *et al.* and that found by the writer for Comet Bennett is related to a difference in the structure of the main tails. From Fig. 1 of Ershkovich *et al.* it can be seen that the tails appear diffuse. This is confirmed for Comet 1973 XII by our Curtis Schmidt plates taken on 7 nights between 1973 December 1 and 1974 January 27; on only one night were rays in the main tail visible. The main tail of Comet Bennett was dominated by 2–5 rays on 8 of the 9 nights.

2.2 Tail Activity

Miller (1972) called attention to the absence of any obvious response of the plasma tail of this comet to phenomena associated with the major geomagnetic storms of 1970 March 8 (discussed in 104 papers in World Data Center A UAG-12 1971). A fairly complete panoply of solar and interplanetary events of the kinds proposed as influences on cometary plasma tails was observed, and one is reminded of a conversation between two well-known fictional characters: (Watson) "The dog did nothing in the nighttime." (Holmes) "That was the curious incident." (*Silver Blaze*, Arthur Conan Doyle).

Our observations of this period of relatively passive tail behavior can be supplemented by reproductions of plates made with the Hamburg Schmidt at the Boyden Observatory by Bester on March 13, 17, 19, and 21 (Bester 1970). In these illustrations the main plasma tail resembles its appearance on our plates. (The contrast is insufficient to show possible faint side rays.) No reports have been published of disturbances on March 15 or 20; it is of course possible that they passed unnoticed. We, thus, have a period of 15 nights (March 7–21) when the record of the main plasma tail shows no indications of major disruptions.

TABLE 2. Major disruptions.

Date	Helio-	References
	graphic	
Date	Lat.	References
March 30	25°	Jockers and Lust 1973
April 4	37	Jockers and Lust 1973; Burlaga <i>et al.</i> 1973
April 9	50	Saito and Oki 1989

The rays that define the main tail of Comet Bennett were typically somewhat sinuous and fragmented on a scale of about 500 Mm on our plates. The absence of major disruptions is in contrast with the well-documented behavior of Comet Halley in its last apparition. Some of these disturbances have been correlated with crossings of the interplanetary neutral sheet (Brandt & Niedner 1987) which, near minimum of solar activity, is encountered at low heliographic latitudes. The latitude of Comet Bennett, on the other hand, varied from -50° at the start of our observations to -15° at the end. But this was at a time near the maximum of solar cycle 20. If the structure of the neutral sheet in that cycle qualitatively resembled that of cycle 21 (Hoeksema 1989) it may have made excursions into high latitudes. Jokipii & Thomas (1981) developed a model for the modulation of galactic cosmic rays by an inclined neutral sheet; it predicts a decrease in neutron counts with increasing inclination. Their Fig. 7 shows that the Climax neutron monitor counts were at a minimum in 1970, consistent with high neutral sheet inclination.

Three disruptions of the tail of Comet Bennett were observed from March 30 to April 9 (Table 2), of which the first two are included by Niedner (1982) in his catalog of possible disconnection events. It is possible that the "quiet time" of March 7–21 when the comet was in negative heliographic latitude compared to the disturbed period March 30–April 9 when the latitude was positive may be attributed to the complex structure of the IMF near solar maximum.

3. THE SIDE RAYS

The side-ray systems of Comet Bennett bear little resemblance to that of Comet 1957 V on 1957 August 22 (Miller 1988, Figs. 1,2). The latter consisted of a set of closely packed, nearly parallel, narrow rays, whereas in Comet Bennett the side-ray features are irregularly spaced, and frequently appear in subsets of diffuse or barely resolved structures with widths (measured near the middle of the observable lengths) of 60–100 Mm. The ray system of March 16 [Fig. 1 (Plate 97)] is a good example. Possibly the system of Comet 1957 V was associated with the disruptive event of the following day (Kearns 1958); Niedner & Brandt (1979) suspected that formation of turning tail rays is strongest at the time of a disconnection event.

3.1 Delineation

Features were delineated by the method employed for Comet 1957 V (Miller 1988). An average of 4 contrasty 8×10 prints at magnifications from 1 to 10 was made for each of the 14 plates selected for study.

A precise 5 mm resseau was contacted around the margins of each enlargement to permit evaluations of paper distortions; the scale parallel to the short side of the prints is 1% greater than that parallel to the long dimension, comparable to a systematic effect found for the paper prints of the Palomar Sky Survey. We have also looked for distortion arising in the enlargement process, and find it insignificant.

The principal uncertainty in the delineation of the rays arises from the exercise of judgement in choosing the central axes of the features. This has been assessed by comparing independent delineations on the same print in different years, and on prints at different magnifications in the same measuring period. The uncertainty in the positions of rays in the coordinate perpendicular to the tail axis is of the order of 5 Mm.

The inventory of delineated features excludes those that were too short to be useful or too faint to be measured satisfactorily. Rays could seldom be traced closer than 100 Mm to the nucleus, and maximum lengths rarely exceeded 2000 Mm.

The rays are either gently curved or sensibly straight. Rather than present graphs or tables of coordinates, we have thought it most convenient for whatever use others may make of the data to tabulate for each feature a quadratic ($Y = A + BX + CX^2$) or the corresponding linear form, in which X is distance from the nucleus, positive antisunward, and Y is positive on the trailing side of the axis (Table 3). These parameters represent the form of the feature between $X(\min)$ and $X(\max)$, and should not be used outside that range. For several rays, sinuosity made it advisable to tabulate the coordinates of a series of points, sufficient in number and spacing to display the undulations (Table 4). In these tables features are each designated by a number corresponding to the March date, and a letter, starting with "A" for the ray most distant from the axis.

3.2 Symmetry about the Tail Axis?

The conventional description of a side-ray system depicts it as roughly symmetrical, with rays sometimes in well-matched pairs; Wurm & Maffei (1961, Figs 1,2) and Moore (1991, Fig. 1) are examples of observed pairs. Our photographs of Comet Bennett are not well suited for comparison with this conventional picture—the trailing side of the axis is dominated by the image of the dust tail. A photored plate (103a-F/RG1) taken on March 18 was analyzed by Sekanina & Miller (1973); their Fig. 2 compares observed and theoretical isophotes. On that diagram the main plasma tail axis lies 15° clockwise of the vertical axis, and it can be seen that the isophotes spread further to the trailing side than to the leading. Only 12 rays certainly not associated with the main tail are seen on our plates on that side.

On March 9, 11, and 16 there are 2, 3, and 5 rays, respectively, on the trailing side of the axis, admittedly a frail set of data on which to base the following discussion. If the ray systems on the trailing and leading sides of the axis were symmetrical about it (not necessarily in matched pairs) we should expect that the slopes of rays with respect to the axis would depend in the same way on position in their respective X, Y half-planes.

For each of the three dates a transparent overlay was made of the trailing rays reflected about the axis, and superposed on the array on the leading side. The overlay was then rotated about the nucleus to bring the two arrays into coincidence (slope as function of the coordinates). The amount of rotation is, with so few trailing rays, very much a matter of judgement; repetitions of the trials indicated an uncertainty of about 2° . The mean absolute rotation, weighted by the number of trailing rays per date was 5° , two rotations in one direction and one in the other. There must be a contribution to this mean from the errors in the adopted position angles of the tail axes, since they enter here with double effect.

The rather weak thrust of this exercise is that there is no conspicuous difference in the configurations of the arrays on opposite sides of the tail axis.

3.3 The Ensemble of the Ray Systems

Side rays are considered by some to be the visible tracers of flow of plasma through magnetic flux tubes. The degree of stability of the interaction of the solar wind and its entrained magnetic field with the comet during our observing period should therefore be indicated by comparison of the arrays on the several dates. If it is quite stable, slopes of rays with respect to the tail axis would depend on position in the X, Y plane in much the same way from date to date.

To look for evidence on this point we estimate the amount of bodily rotation of each day's array to bring it into agreement with a mean orientation representative of all dates. For this we deal only with rays on the leading side of the axis. Three independent judgements were made of each rotation angle, yielding an overall average deviation of $\pm 1^\circ$ for a single estimate.

On 7 of the 9 nights the orientations of the individual arrays are scattered about the mean with an average deviation of $\pm 2^\circ$. Taking into account the uncertainty in the adopted position angles of the tail axes and the uncertainty in the size of the rotations, the structure of the side-ray systems on these dates can be considered to follow a uniform pattern. On March 11 and 12 the deviations from the mean orientation are substantially greater, $+9^\circ$ and -13° , respectively. Inspection of the images of the main tail and side-rays reveals no unusual characteristics; on both dates the adopted position angle of the axis depends on that part of the main tail lying beyond the side-rays, and it is possible that the inner segment of the axis is not aligned with its outer extension.

TABLE 3. Ray parameters (except sinous rays) (Mm).

Ray	A	B	$\alpha \times 10^4$	X(min)	X(max)	Notes	Ray	A	B	$\alpha \times 10^4$	X(min)	X(max)	Notes
7A	-92	-0.696	3.730	200	530	7	12E	-67	-0.262	-	970	2620	5
7B	-61	-0.641	2.924	150	690	-	12F	-	-	-	-	-	1, 4
7C	-78	-0.440	0.808	210	840	-	14A	-248	-1.031	-	30	220	-
8A	-79	-0.484	-	150	520	7, 10	14B	-184	-0.843	3.471	90	280	-
8B	-105	-0.231	-2.426	270	610	-	14C	-152	-0.668	-	140	400	-
8C	-26	-0.256	-	740	1260	-	14D	-29	-0.756	1.569	260	820	9
8D	-18	-0.180	0.231	980	2790	4, 6	14E	50	-0.513	0.735	890	2050	9
9A	-113	-1.048	9.804	20	270	-	14F	64	-0.365	0.342	1260	2620	9
9B	-67	-0.789	3.927	110	590	-	14G	-68	-0.179	-	1710	2880	-
9C	-69	-0.552	1.077	100	620	-	14H	57	-0.180	-	2090	2980	4
9D	-8	-0.659	3.059	270	600	-	16A	-167	-1.118	6.822	20	160	-
9E	-41	-0.441	0.899	190	580	-	16B	-127	-1.032	5.526	70	400	-
9F	-40	-0.291	-	180	1230	-	16C	-118	-0.676	-	150	310	6
9G	-23	-0.281	-	620	1480	-	16D	-54	-0.568	0.649	210	1300	-
9H	-34	-0.221	-	920	1980	4	16E	-36	0.491	0.351	380	1610	-
9I	91	0.651	-5.235	60	360	2	16F	-58	-0.359	-	610	1790	-
9J	60	0.548	-3.222	120	620	2	16G	-	-	-	-	-	1, 11
10A	-59	-0.677	3.050	140	500	-	16H	-	-	-	-	-	1
10B	-48	-0.549	1.641	240	860	-	16I	-	-	-	-	-	1
10C	-44	-0.428	0.904	360	1320	-	16J	-605	0.156	-0.310	2890	4790	-
10D	-64	-0.207	-	730	1900	7	16K	-	-	-	-	-	1
10E	61	0.647	-2.742	230	660	2	16L	184	1.179	-19.442	80	210	2
11A	-154	-0.614	-	60	220	-	16M	166	0.578	-	150	370	2
11B	-117	-0.500	-	120	320	-	16N	67	0.572	-1.672	240	910	2
11C	-89	-0.485	1.632	190	790	-	16O	80	0.360	-	480	990	2
11D	-78	-0.283	0.393	600	1400	7	16P	-6	0.486	-0.949	770	1330	2
11E	-116	-0.106	-	720	1520	4	18A	-269	-1.279	19.422	-56	120	-
11F	3	-0.125	-	1430	2240	4	18B	-116	-0.809	2.601	99	408	-
11G	112	1.230	-22.929	70	200	2	18C	-102	-0.614	1.147	130	1060	-
11H	89	0.540	-1.783	140	610	2	18D	-85	-0.449	0.315	460	1220	6
11I	90	0.421	-0.864	140	770	2	18E	-138	-0.314	-	1030	1360	-
12A	-105	-0.716	-	140	440	-	18F	-108	-0.300	-	780	1450	-
12B	-55	-0.689	-	250	440	-	18G	32	0.517	-2.777	280	540	2, 10
12C	18	-0.717	-	320	660	-	18I	70	0.116	-	840	1510	2, 3
12D	50	-0.573	-	560	1050	8	18J	32	0.108	-	770	1270	2, 3
12D2	-	-	-	-	-	1, 8							

Notes to Table 3

- 1) See Table 4
- 2) On trailing side of tail axis
- 3) Component of main tail?
- 4) Close double
- 5) Outer component of close double
- 6) Broad, diffuse
- 7) Component of diffuse feature
- 8) Narrow dark lane between two features
- 9) Inner edge of diffuse feature
- 10) Outer edge of diffuse feature
- 11) Center of partially resolved feature

TABLE 4. Sinuous rays (Mm).

X	Y	X	Y	X	Y	X	Y
Ray 12D2		Ray 16G		Ray 16H		Ray 16K	
700	-260	800	-280	1400	-320	3700	-300
1100	-440	1000	-340	1600	-370	4000	-380
1500	-610	1200	-400	1800	-400	4300	-420
1800	-730	1600	-510	2000	-420	4600	-440
2200	-840	2000	-630	3000	-610	4900	-480
Ray 12F		2400	-750	3400	-670	5100	-520
1600	-340	3000	-880	3800	-710	5400	-560
2100	-460	3800	-1010	4400	-820	5800	-580
2500	-520	4400	-1120	Ray 16I			
3300	-600	4800	-1170	2800	-450		
3700	-640	5200	-1240	3800	-570		
4000	-690	5600	-1330	4400	-650		
4300	-750	6000	-1390	4800	-710		
4600	-780	7000	-1530	5200	-760		
5000	-790			5700	-800		

3.4 Kinematics

The only well-established kinematic property of featureless tail rays is folding to the axis with decreasing angular velocity (Wurm 1963). On each of 5 nights 2 plates of Comet Bennett were taken at intervals of 14 to 38 minutes. These intervals are too brief to permit definitive measurement of the rates of ray closing; we wish to ask only if the rays of Comet Bennett appear to conform to Wurm's classical description.

During these short intervals the ray motion appears as a self-parallel displacement; similar behavior can be seen in Fokker's diagram of the folding rays of Comet Brooks 1911 V (Fokker 1953, Fig. 3) and Lüst's of Comet Morehouse 1908 III (Lüst 1967, Fig. 3). We have therefore adopted as a measure of ray motion the displacement perpendicular to the ray in velocity units. The uncertainty of a velocity due to all contributing errors is estimated as ± 10 km/s. In Table 5 are the displacements of 22 rays selected as being suitably well-defined for measurement. All velocities are directed toward the axis, and for the most part decrease with decreasing axial distance, the notable exceptions being the three innermost rays of March 16. These velocities would make insignificant contributions to the widths of rays as seen at the scale of our plates.

4. COMPARISON WITH MAGNETICALLY CHANNЕLED OUTFLOW

In this section we compare our observations with a model of magnetically channeled outflow (MCO) in which the description of Wurm (1963) is explained by Alfvén's theory (Alfvén 1957) combined with flux ropes (Parker

TABLE 5. Closing velocities of rays (km/s).

Ray	Vel.	Ray	Vel.	Ray	Vel.
March 8		March 12		March 16	
8A	46	*12B,C	54	16A	18
8B	48	*12D1,D2	34	16B	16
8C	31	12E	19	16C	4
8D	7	12F	0	16D	13
March 11		March 14		March 16	
11C	20	14A	30	16E	10
11D	11	14B	15	16G	15
11E	14	14C	10		
11F	3	14D	6		

* Close pair of rays

1979; Wolff *et al.* 1985) to produce flow of plasma in discrete rays. We are aware that others do not consider rays as tracers of magnetic fields.

4.1 Projection into the Plane of the IMF

An observed side-ray system is the projection on the sky of a three-dimensional array that, in a simple version of the MCO model, is confined to the plane of the IMF defined by the Sun-Comet vector and that of constant heliographic latitude at the comet. To test this hypothesis we have selected a standard array consisting of rays 18A, 16A, 18C, 16D, 16F, and 16G reduced to a common axis orientation (Sec. 3.3). This set of rays was projected into the IMF plane of each date. Figures 2(a) and 2(b) are plots of these rays as seen on the plane of the sky, and Figs. 2(c), 2(d), and 2(e) shows the projections into the IMF planes of a sample of three nights.

The patterns of the projected arrays from March 7 to 11 do not do great violence to one's conception of what a side-ray system "ought" to look like, if one is guided by Wurm's description, distilled from the variety of observations upon which he based it. But from March 12 to 18 the projected arrays become progressively less acceptable. Inasmuch as the angles between the planes of the sky and the IMF increase from 76° on March 7 to 86° on the 18th, the writer believes that the projections, exhibiting as they do a regular progression in structure with date, are an artifact of the projection geometry. It also strikes one as improbable that an evolution in ray structure illustrated in Figs. 2(c) and 2(e) would replicate on each date the configuration on the sky shown in Figs. 2(a) and 2(b).

The choice adopted above of a single plane for the IMF and side rays was chosen after considering complicating circumstances. Analysis by Brandt *et al.* (1973) indicated a meridional component of the solar wind flow, and three-dimensional studies of cometary magnetospheres lead to the expectation that field lines may slip up and over the cometopause in the manner illustrated graphically by Saito

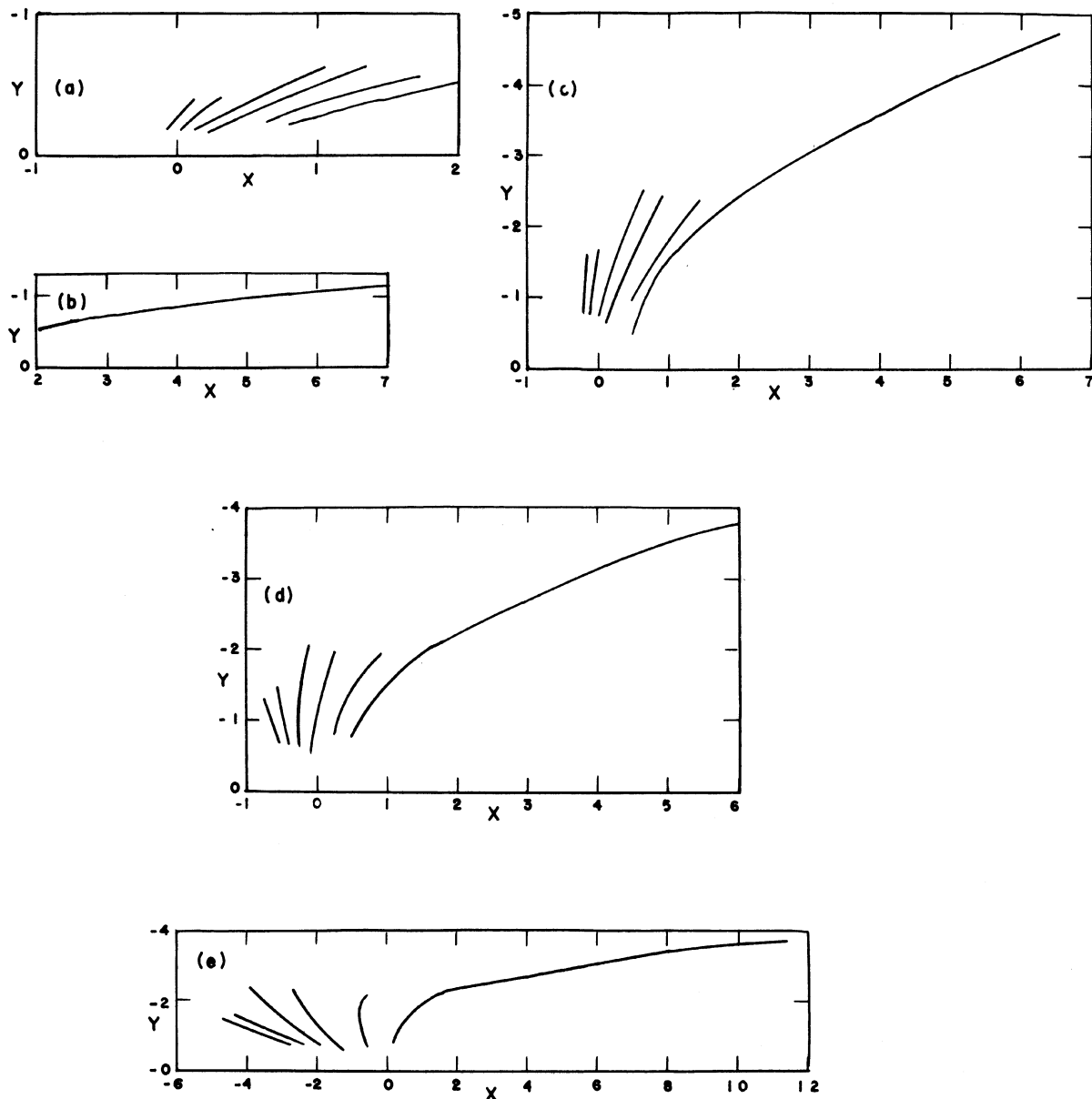


FIG. 2. Standard array of side rays. (a) On plane of sky, Ray 16G to 2000 Mm. (b) Ray 16G 2000-7200 Mm on plane of sky. (c)-(e) Projected into plane of IMF on March 7, 12, and 18, respectively. Note different scales, unit of distance is 10^6 km.

et al. (1987, Fig. 2). In view of the drastic distortions of the form of observed rays projected into slightly modified orientations of the IMF plane as described below, it would be premature to venture on elaborations of the MCO model employed here. Study of comets for which the viewing geometry is more favorable than in the present case is in progress, and may provide a guide to modifications of the model.

To test the influence of small variations in the orientation of the IMF plane we have carried out projections into four planes of which the perpendiculars were displaced by 10° to heliographic north, east, south, and west. The projected arrays for northward displacement are plausible for

all dates except March 18, and those to westward with the exception of March 16 and 18. Projections to east and south are increasingly unrealistic with progression in date. Figure 3 presents the projected arrays for March 12.

We conclude that by trial and error one might find tilted planes giving acceptable arrays for each date, but that in the absence of observations of the high-latitude structure of the IMF in March 1970 this would be a sterile exercise.

4.2 The Influence of Discontinuities in the IMF

Schmidt (1974) pointed out that cometary streamers and tangential discontinuities in the IMF have occurrence

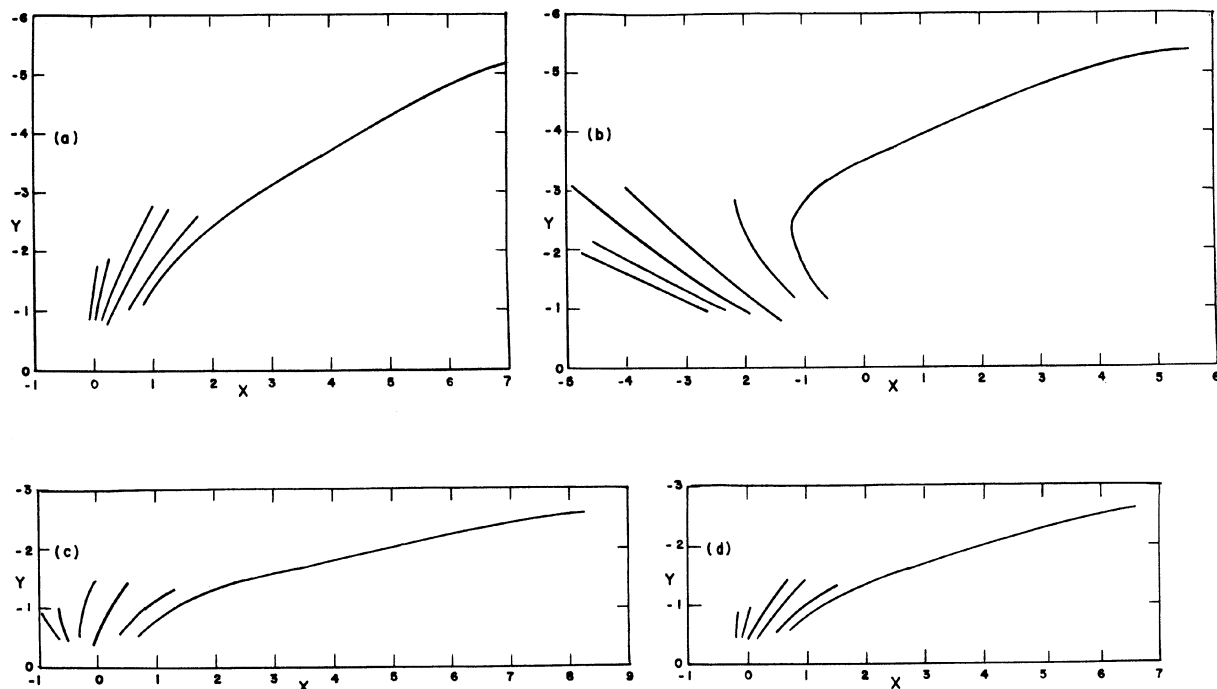


FIG. 3. (a)–(d) Standard array projected into planes inclined 10° to north, east, south, and west, respectively, with respect to plane of IMF on March 12. Note different linear scales, unit of distance is 10^6 km.

rates of about 1 per hour, and suggested that discontinuities might be the cause of rays. Schmidt & Wegmann (1982), Fedder *et al.* (1984), Huebner *et al.* (1989), and Schmidt-Voigt (1989) have investigated the generation of tail structures by 90° and 180° rotations of the field, but did not address the formation of regular sequences of side rays. Jockers (1982) remarked that formation of these ray sequences, such as that of Comet 1969 IX (Miller 1979) by a randomly turning field seemed difficult. In the context of the present investigation we should expect that discontinuities in the IMF would degrade the familiar inverse correlation between the length of a side ray and its distance from the axis (Wurm 1963, Fig. 1).

Rays fade out gradually with distance from the nucleus, making measurement of length impractical. We therefore adopt Kendall's rank correlation coefficient τ (Kendall 1962); rays were ranked in order of distance from the axis, and in order of length on our prints, omitting those appreciably fainter than the typical member of an array. We calculated the τ 's of the observed arrays on the leading side of the axis for each date, and also for those on the following side on March 11 and 16 (Table 6). For 8 of the 11 arrays, the correlation coefficients are 1.

What is the probability of the observed set of τ 's if, instead of the members of an array being confined to a single plane, successive three-dimensional rays trace IMF lines lying in planes random walked in azimuth about the sun-comet line by tangential discontinuities?

For each observed array we set up a "proxy" array which corresponds to the observed only in the number of rays, which were assumed to be rectilinear. To derive an

empirical expression for the lengths of the rays, we plotted X_{\max} (Table 3) against the mean slopes of the delineated segments for 44 rays. The plotted points form two surprisingly tight correlations for March 7–11 and 12–18, respectively, with no overlap. To convert slope to time we adopted Wurm's law (Wurm & Mammano 1972) for rate of change of slope as function of slope. The resulting mean growth rates parallel to the X axis are 59 and 77 km/s, respectively, for the two groups of dates.

Although the mean errors of the rates are about 10%, note that the tabulated values of X_{\max} represent the measurable tips of ray images on our prints, and are not the results of applying photometric criteria to the images on the plates. We also are aware that it is inconsistent to make use of Wurm's law derived from rays projected on the sky to set up our three-dimensional proxy arrays. We therefore stress that the growth rates quoted above are not to be given any weight as determinations of physical growth rates.

In each proxy array the ray most distant from the axis was assigned a slope of 60° (a judgement based on observed arrays) and an arbitrary length of 500 Mm. The remaining rays were assumed to have been generated at successively earlier 1-h intervals, the slopes were derived from Wurm's law, and lengths increased at a rate of $77 \text{ km/s}/\cos(\text{slope})$.

The shortest ray in each proxy array was assigned a plane of which the azimuth about the Sun-Comet line was chosen at random. For each succeeding ray the plane was random walked through an angle for which we constructed a probability distribution from observations of tangential

TABLE 6. Anticorrelation between ray length and distance from axis.

March			
Date	N	τ	$P(\tau)$
7	3	1	0.39
8	3	1	0.39
9	7	0.67	0.50
10	4	1	0.19
11	4	1	0.22
11*	3	1	0.37
12	6	0.93	0.04
14	7	1	0.06
16	10	0.73	0.24
16*	5	1	0.08
18	6	1	0.03

Notes to Table 6

N: number of rays

*: array on trailing side of tail axis

 τ : Kendall's rank correlation coefficient $P(\tau)$: probability that τ equal or exceed
observed value

discontinuities by Mariani *et al.* (1983, Fig. 6) and Leping & Behannon (1986, Fig. 10). The proxy ray was then projected into the sky plane; if the angle between the projected ray and the projected Sun–Comet line (considered to be the observed tail axis) was less than 5° , it was assumed that the ray would have been identified as part of the main tail, and the ray plane was further randomized until a larger projected angle was obtained. The correlation coefficient for the projection of the array was computed, and randomizing of the proxy array was repeated 1000 times to obtain a probability distribution of τ . From this distribution we read the probability that, given the characteristics of the proxy array, we should find an observed τ equal to or exceeding that in Table 6. If the observed τ equaled 1, we have conservatively taken the probability that τ equal or exceed 0.9. The probabilities are in the last column of Table 6.

As a check on these calculations, another set was made in which cases were rejected when the angles between the projected ray and tail axis were less than 10° , and the angle of the line of sight to the Sun–Comet line was assumed to be 90° (true angles were equal to or exceeded 75°). The resulting probabilities of the observed τ 's are in good agreement with the first set, and are not referred to in the following discussion.

The probabilities in Table 6 do not exclude the possibility that any single one of the observed arrays could be

generated by a model in which the planes of the proxy arrays were random walked about the tail axis in a manner consistent with the observed frequencies of tangential discontinuities in the IMF. But the continued product of the six largest probabilities is 0.001, and of all eleven is 2×10^{-9} . We conclude that the configuration of the ensemble of the eleven observed arrays is inconsistent with such a model.

4.3 The Influence of the Winding Angle of the IMF

At the heliocentric distances (0.61–0.54 AU) and heliographic latitudes (-50° to -15°) of Comet Bennett, the winding angles (WA) of the Parker IMF spiral (Parker 1958) with an arbitrarily chosen solar wind velocity of 400 km/s range from 23° to 29° on the trailing side of the axis, and from 157° to 151° on the leading side. Smith & Bieber (1991) suggest that the WA of the polar field may be approximately 5° rather than zero, so the computed WAs may be somewhat smaller than the true values.

We are not aware of any MHD models of IMF lines at such extreme WAs which could be compared with the observed rays of Comet Bennett, or with their projections into the IMF plane. Wegmann *et al.* (1987, Fig. 4) and Huebner *et al.* (1989, Fig. 3) illustrate the effects of WAs of 47° and 57° , respectively. Both diagrams show a tendency for the field lines to become convex to the axis at distances from the nucleus within the range of our observations, but we do not see this phenomenon in our observations.

A priori one might expect that WAs appropriate to Comet Bennett would lead to an asymmetry in the structure of the ray systems on opposite sides of the tail axis. In Sec. 3.2 we found that, based on only 10 trailing rays, there is no marked difference of the kind expected. It would be of great interest to see theoretical predictions of IMF lines draped about the nucleus for comets such as Bennett, 1957V, and 1969 IX. On dates when side rays were seen at the two latter comets (Miller 1988, 1979) the WAs were 23° and 22° , respectively. Unfortunately, the comets appeared near maxima of solar activity, and it is doubtful that it is now possible to reconstruct the orientation of the IMF at high latitudes.

4.4 Conclusions

The object of the work described in this section was to investigate the compatibility of our observations of side-rays with simple models of magnetically channeled plasma flow, and to suggest the desirability of additional observations and theoretical modeling of draped field lines for extreme winding angles.

In Sec. 4.1, projecting the observed rays into the ideal plane of the IMF, we find the resulting ray configurations unacceptable as representations of physically plausible arrays. We intend to apply similar analyses to cases in which the angles between the planes of the sky and the IMF are smaller, and thus more favorable, than in the case of this comet. The influence of tangential discontinuities in the

IMF on the observed anticorrelation between the distance of a ray from the tail axis and its length is examined in Sec. 4.2. The probability of simultaneous occurrence of the 11 observed correlations (average value 0.94) in a model in which the planes of successively formed rays are random walked about the Sun–Comet radius vector by tangential discontinuities in the IMF is so small that this modification of the MCO model appears to be ruled out. In Sec. 4.3 we call attention to the small (large) winding angles of the

Parker spiral IMF on the trailing (leading) sides of the tail axis of this comet, and to the lack of theoretical calculations of IMF field lines draped about the nucleus under such circumstances.

The Curtis Schmidt plates were taken by Arturo Gomez of the CTIO staff under the terms of the agreement governing the loan of the telescope to AURA. The writer is grateful to A. Gomez for the quality of his work.

REFERENCES

- Alfvén, H. 1957, *Tellus*, 9, 92
 Bester, M. J. 1970, *IrAJ*, 9, Plates VI, VIII, IX, X
 Brandt, J. C., Harrington, R. S., & Roosen, R. G. 1973, *ApJ*, 184, 27
 Brandt, J. C., & Niedner, M. B., Jr. 1987, in *Explorations of Halley's Comet*, edited by M. Grewing, F. Praderie, and R. Reinhard (Springer, New York), p. 281
 Burlaga, L. F., Rahe, J., & Donn, B. 1973, *Solar Phys.*, 30, 211
 Ershkovich, A. I., Niedner, Jr., M. B., & Brandt, J. C. 1982, *ApJ*, 262, 396
 Fedder, J. A., Brecht, S. H., & Lyon, J. G. 1984, *Naval Research Lab. Memo. Report No. 5306*
 Fokker, A. D., Jr. 1953, in *La Physique des Cometes* (University of Liège, Liège), p. 201
 Hoeksema, J. T. 1989, *Adv. Space Res.*, 9, (4), 141
 Huebner, W. F., Boice, D. C., Schmidt, H. U., Schmidt-Voigt, M., Wegmann, R., Neubauer, F. M., & Slavin, J. A. 1989, *Adv. Space Res.*, 9, (3), 385
 Ioffe, Z. M. 1985, *SvA*, 31, 73
 Ip, W. H. 1980, *A&A*, 92, 95
 Jockers, K. 1982, in *Need for Coordinated Ground-Based Observations of Halley's Comet*, edited by P. Véron, M. Festou, and K. Kjær (European Southern Observatory, München), p. 193
 Jockers, K., & Lüst, R. 1973, *A&A*, 26, 113
 Jokipii, J. R., & Thomas, B. 1981, *ApJ*, 243, 1115
 Kearns, C. 1958, *PASP*, 70, 202
 Kendall, M. G. 1962, *Rank Correlation Methods*, 3rd ed. (Hafner, New York)
 Lepping, R. P., & Behannon, K. W. 1986, *J. Geophys. Res.*, 91, 8725
 Lüst, R. 1967, *ZfA*, 65, 236
 Mariani, F., Bavassano, B., & Villante, U. 1983, *Solar Phys.*, 83, 349
 Miller, F. D. 1972, *BAAS*, 4, 425
 Miller, F. D. 1979, *Icarus*, 37, 443
 Miller, F. D. 1988, *AJ*, 95, 553
 Miller, F. D., & Liller, W. 1986, in *ESLAB Symposium No. ESA SP-250*, Vol. 3, edited by B. Battrock, E. J. Rolfe, and R. Reinhard, p. 137
 Moore, E. P. 1991, *A&A*, 247, 247
 Niedner, Jr., M. B. 1982, *ApJS*, 48, 1
 Niedner, Jr., M. B., & Brandt, J. C. 1979, *ApJ*, 234, 723
 Niedner, Jr., M. B., Ershkovich, A. I., & Brandt, J. C. 1983, *ApJ*, 272, 362
 Niedner, Jr., M. B., Rothe, E. D., & Brandt, J. C. 1978, *ApJ*, 221, 1014
 Parker, E. N. 1958, *ApJ*, 128, 664
 Parker, E. N. 1979, *Cosmical Magnetic Fields* (Clarendon, Oxford), Chap. 9
 Saito, T., & Oki, T. 1989, in *Proceedings of the 2nd International Workshop on Relation Between Laboratory and Space Plasma*, edited by H. Kikuchi (Springer, New York), p. 531
 Saito, T., Saito, K., Aoki, T., & Yumoto, K. 1987, *A&A*, 187, 208
 Schmidt, H. U. 1974, *MitAG*, 35, 248
 Schmidt, H. U., & Wegmann, R. 1982, in *Comets*, edited by L. L. Wilkening (University of Arizona Press, Tucson), p. 538
 Schmidt-Voigt, M. 1989, *A&A*, 210, 433
 Sekanina, Z., & Miller, F. D. 1973, *Sci*, 179, 565
 Smith, C. W., & Bieber, J. W. 1991, *ApJ*, 370, 435
 Wegmann, R., Schmidt, H. U., Huebner, W. F., & Boice, D. C. 1987, in *Physical Processes in Comets, Stars, and Active Galaxies*, edited by W. Hillebrandt, E. Meyer-Hoffmeister, and H. C. Thomas (Springer, New York), p. 34, Fig. 4b
 Wolff, R. S., Siscoe, G. L., Sibeck, D. G., & Neugebauer, M. M. 1985, *Geophys. Res. Letts.*, 12, 749
 Wurm, K. 1963, in *The Solar System*, Vol. 4, *Moon, Meteorites, & Comets*, edited by B. M. Middlehurst and G. P. Kuiper (University of Chicago Press, Chicago), p. 573
 Wurm, K., & Maffei, P. 1961, *ZfA*, 52, 294
 Wurm, K., & Mammano, A. 1972, *Ap&SS*, 18, 273

